

# Dalton Transactions

Accepted Manuscript



This article can be cited before page numbers have been issued, to do this please use: A. P. Chattopadhyay and P. Mandal, *Dalton Trans.*, 2015, DOI: 10.1039/C5DT01260K.



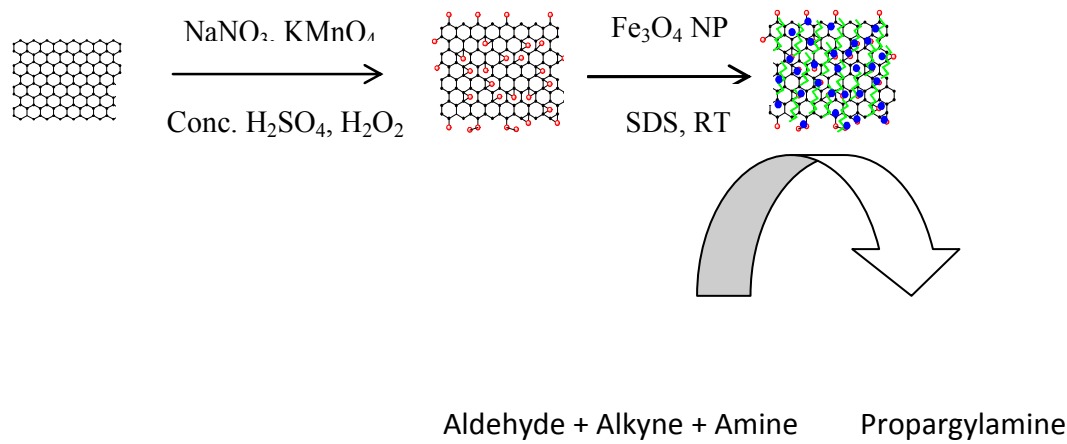
This is an *Accepted Manuscript*, which has been through the Royal Society of Chemistry peer review process and has been accepted for publication.

*Accepted Manuscripts* are published online shortly after acceptance, before technical editing, formatting and proof reading. Using this free service, authors can make their results available to the community, in citable form, before we publish the edited article. We will replace this *Accepted Manuscript* with the edited and formatted *Advance Article* as soon as it is available.

You can find more information about *Accepted Manuscripts* in the [Information for Authors](#).

Please note that technical editing may introduce minor changes to the text and/or graphics, which may alter content. The journal's standard [Terms & Conditions](#) and the [Ethical guidelines](#) still apply. In no event shall the Royal Society of Chemistry be held responsible for any errors or omissions in this *Accepted Manuscript* or any consequences arising from the use of any information it contains.

An easy-to-prepare Fe<sub>3</sub>O<sub>4</sub>-graphene oxide nanocomposite which works well as reusable catalyst for A<sup>3</sup>-coupling reaction



Cite this: DOI: 10.1039/c0xx00000x

www.rsc.org/xxxxxx

## ARTICLE TYPE

# Excellent catalytic activity of magnetically recoverable Fe<sub>3</sub>O<sub>4</sub>-graphene oxide nanocomposites prepared by a simple method

Prasenjit Mandal and Asoke P. Chattopadhyay\*

*Received (in XXX, XXX) Xth XXXXXXXXX 20XX, Accepted Xth XXXXXXXXX 20XX*

DOI: 10.1039/b000000x

Fe<sub>3</sub>O<sub>4</sub>-graphene oxide nanocomposite has been synthesized *via* a chemical reaction with magnetite particle size of 18-25 nm. The resulting nanocomposite can be easily manipulated by an external magnetic field, exhibit excellent catalytic activity and may be reused for several cycles with marginal loss of activity. This recyclable nanocomposite provides an efficient, economic, novel route for multi-component A<sup>3</sup> coupling reaction of aldehyde, amine and alkyne and gives the propargylamine in excellent yields.

## 10 Introduction

The highly efficient multi-component reactions in one-pot syntheses play an important role in current organic synthesis<sup>1</sup> since they not only exhibit selectivity and higher atom economy, but allow construction of molecules of more diversity and complexity and are thus highly valued among synthetic methodologies. Furthermore, in many cases, multi-component reactions are easy to perform leading to simple experimental procedures as well as lower cost, time and energy. The catalytic coupling reaction of aldehyde, amine and alkyne (A<sup>3</sup> coupling) is one of the best examples, where propargylamine is obtained as the major product. During the past decade, much effort has been spent to develop one-pot multi-component reactions to make new carbon-carbon bonds.<sup>2</sup> These are typically carried out using a host of stoichiometric reagents and protecting groups, often generating much waste in the process.

Propargylamines are important components of useful synthetic precursors<sup>3</sup> and biologically active compounds.<sup>4</sup> This is reflected in the interest shown in its synthesis.<sup>5-10</sup> The particular coupling reaction (A<sup>3</sup> coupling) can be successful using various types of catalyst such as copper-doped alumina with microwave assistance,<sup>11</sup> copper in solid phase systems,<sup>5</sup> gold,<sup>12</sup> silver,<sup>13</sup> ruthenium-copper cocatalyst<sup>5</sup> and iridium.<sup>10</sup> The last two in the list are toxic in nature and have low turnover numbers in their respective reactions, are difficult to prepare and are not environmentally friendly. Fe<sub>3</sub>O<sub>4</sub> nanoparticles and Fe<sub>3</sub>O<sub>4</sub>-graphene oxide (Fe<sub>3</sub>O<sub>4</sub>-GO) nanoparticle catalysts,<sup>14-15</sup> on the other hand, are prepared from iron-salts and graphite powder, which are both cheap and readily available. They are also moisture-sensitive, and environmentally friendly. Fe<sub>3</sub>O<sub>4</sub> nanoparticles are superparamagnetic, with interesting magnetic and biological activities. Such a novel composite with high specific surface area and strong magnetic sensitivity exhibits

excellent catalytic activity in the A<sup>3</sup>-coupling reaction.

The development of a clean synthetic procedure has become crucial and demanding because of increasing environmental concerns. Heterogeneous organic reactions have many advantages in this respect, such as ease of separation and handling, recycling, and environmentally safe disposal.<sup>16</sup> The heterogeneous catalysts such as graphene oxide-Fe<sub>3</sub>O<sub>4</sub> have attracted a great deal of attention in recent years because of their high catalytic activity and interesting structures.<sup>17</sup> The Fe<sub>3</sub>O<sub>4</sub>-GO magnetic nanoparticles have been most useful as heterogeneous catalysts because of their numerous applications in biotechnology, nanocatalysis, and medicine.<sup>18</sup> In this context the magnetic properties<sup>19</sup> make possible the complete recovery of the catalyst by means of an external magnetic field.<sup>20</sup> On the other hand, performing organic reactions in aqueous media has several benefits because water would be considerably safe, nontoxic and economical compared to organic solvents, abundant, and environmentally friendly. Moreover, water exhibits selectivity and unique reactivity, which is different from those in conventional organic solvents.<sup>21</sup> Therefore, the development of a catalyst that is not only stable toward water but also simply recyclable seems highly desirable.

In continuation of efforts to develop new synthetic methods for the synthesis of propargylamines containing important biologically active compounds,<sup>22</sup> herein we report our contribution to it viz. using GO-Fe<sub>3</sub>O<sub>4</sub> nanocomposites as excellent A<sup>3</sup> coupling catalysts for its production. These materials are robust, inexpensive, and easy to make. They are highly active in the coupling reaction of aldehydes, amines, and alkynes, giving propargylamines selectively with water as the only by-product (Scheme-1). This feature is of importance for purity requirement, especially in pharmaceutical industry. Simple mild and low-cost reusable methods are highly desirable to avoid toxicity.

\*Department of Chemistry, University of Kalyani, Kalyani 741235, India; Email: asoke@klyuniv.ac.in; Fax: +91-33-25828282; Tel: +91-33-25828750

## Experimental

### Materials

Graphite powder (70  $\mu\text{m}$ , Qingdao Graphite Company),  $\text{KMnO}_4$ ,  $\text{FeCl}_3 \cdot 6\text{H}_2\text{O}$ ,  $\text{H}_2\text{SO}_4$ , sodium dodecylsulfate (SDS),  $\text{FeSO}_4 \cdot 7\text{H}_2\text{O}$ , ammonia solution,  $\text{H}_2\text{O}_2$ . All chemicals were reagent grade and purchased from Sinopharm Chemical Reagent Co. Ltd. Milli-Q (Millipore, Billerica, MA, USA) and nanopure (double distilled water, filtered through 200  $\mu\text{m}$  filter) water was used in all experiments.

### Preparation of water-soluble magnetic $\text{Fe}_3\text{O}_4$ nanoparticles

Magnetically active  $\text{Fe}_3\text{O}_4$  nanoparticles were synthesized by chemical co-precipitation of  $\text{Fe}^{3+}$  and  $\text{Fe}^{2+}$  ions in an alkaline solution, followed by a treatment under hydrothermal conditions.<sup>23-24</sup> 5.7 g  $\text{FeCl}_3 \cdot 6\text{H}_2\text{O}$  and 2.7 g  $\text{FeSO}_4 \cdot 7\text{H}_2\text{O}$  were dissolved in 10 mL nanopure water separately. These two solutions were thoroughly mixed and added to 20 mL 10 M ammonium hydroxide with constant vigorous stirring for 1 h to make all materials dissolved completely at 25  $^\circ\text{C}$ . Colour of the solution changes from dark green to black indicating the formation of  $\text{Fe}_3\text{O}_4$  and completion of the reaction. Then the dark black slurry of  $\text{Fe}_3\text{O}_4$  particles was heated at 80  $^\circ\text{C}$  in a water bath for 30 min. The particles thus obtained exhibited a strong magnetic response. Impurity ions such as sulphates and chlorides were removed by washing the particles several times with nanopure water. Then the particles are dispersed in 20 mL nanopure water and sonicated for 10 min at 60 MHz. The yield of precipitated magnetic nanoparticles was determined by removing known aliquots of the suspension and drying to a constant mass in an oven at 70  $^\circ\text{C}$ . The prepared magnetic nanoparticles were stable at room temperature (25-30  $^\circ\text{C}$ ) without getting agglomerated.

### Preparation of graphene oxide

Graphene oxide (GO) was prepared according to the modified Hummers' method from graphite powder.<sup>25</sup> In detail, 1 g of graphite powder and 300 mg of  $\text{NaNO}_3$  in 22 mL of concentrated  $\text{H}_2\text{SO}_4$  were vigorously stirred in an ice bath. 3 g of  $\text{KMnO}_4$  was added gradually with constant stirring, to prevent the temperature of the mixture from exceeding 8-10  $^\circ\text{C}$ . The ice bath was then removed and the mixture was stirred at 30  $\pm$  3  $^\circ\text{C}$  for 35 min. After completion of the reaction, 45 mL of distilled water was added, and the temperature was kept at 95  $^\circ\text{C}$  for 18 min. The reaction was terminated by adding 140 mL of distilled water and 15 mL of 30%  $\text{H}_2\text{O}_2$  solution. The reaction product was centrifuged and washed successively with deionized water and 5% HCl solution repeatedly until sulfate could not be detected with  $\text{BaCl}_2$ . Finally, graphene oxide was obtained after drying under vacuum at 60  $^\circ\text{C}$  for 24 h.

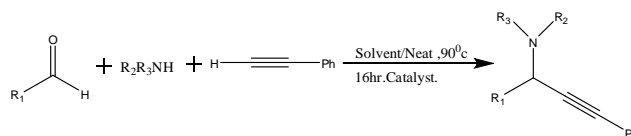
### Preparation of $\text{Fe}_3\text{O}_4$ -GO nanocomposite.

The  $\text{Fe}_3\text{O}_4$ -GO nanocomposite was synthesized by co-precipitation<sup>26</sup> of prepared  $\text{Fe}_3\text{O}_4$  nanoparticle in the presence

of GO in water. SDS was added to the prepared  $\text{Fe}_3\text{O}_4$  nanoparticle, which was then added slowly to the GO solution, along with ammonia solution, with constant stirring for 30 min to make all materials dissolve completely. The temperature was raised to 85  $^\circ\text{C}$ , and a 30% ammonia solution was added to adjust the pH to 10. After being rapidly stirred for 30 min, the solution was cooled to room temperature. The dark black coloured solution was then filtered and washed with Milli-Q water/ethanol and dried in vacuum at 70  $^\circ\text{C}$ . In this powdered  $\text{Fe}_3\text{O}_4$ -GO nanocomposite, the weight ratio of  $\text{Fe}_3\text{O}_4$  to GO was 2:1. (See Scheme 1)

### Typical procedure for the $\text{A}^3$ coupling reaction

The reactions were carried out under conventional heating in a conventional round bottomed flask (rbf), under constant stirring. The typical  $\text{A}^3$  coupling reaction was performed as follows. 0.50 mmol aldehyde, 0.60 mmol amine and 0.75 mmol alkyne were taken in a 50 ml rbf with 6 ml water. 0.05 mmol catalyst was added to it. The reaction mixture was stirred for 16 h at 80- 90  $^\circ\text{C}$ . Progress of the reaction was monitored by sampling aliquots of reaction mixture and subsequent analysis by GC/GC-MS (VB-1 column, FID), and/or purified by column chromatography (hexane, silica gel:EtOAc = 4:1). Product identity and purity were confirmed by  $^1\text{H}$  NMR spectroscopy and GC-MS spectrometry. (Scheme 2)



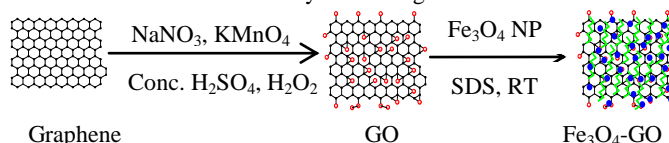
Conditions: aldehyde (1 eq.), amine (1.2 eq.), alkyne (1.5 eq.),  $\text{GO-Fe}_3\text{O}_4$  (50 mg, 0.3 mol%  $\text{Fe}_3\text{O}_4$  NP) in 5 mL solvent or neat for 16 h, temperature above 90  $^\circ\text{C}$ ; conversions were determined by GC-MS and  $^1\text{H}$  NMR of crude reaction mixture.

## Results and discussion

### Characterization

All synthesized nanoparticles were characterized in the usual manner, viz. powder XRD, FT-IR, SEM, TEM, thermogravimetric analysis (TGA) and Raman Spectroscopy.

Available data for different systems are given below.



Graphene

GO

$\text{Fe}_3\text{O}_4$ -GO

Scheme 1. Synthesis of  $\text{Fe}_3\text{O}_4$ -GO nanocomposites. Red dots indicate oxygen atoms, blue dots indicate  $\text{Fe}_3\text{O}_4$  nanoparticles, green lines represent SDS.

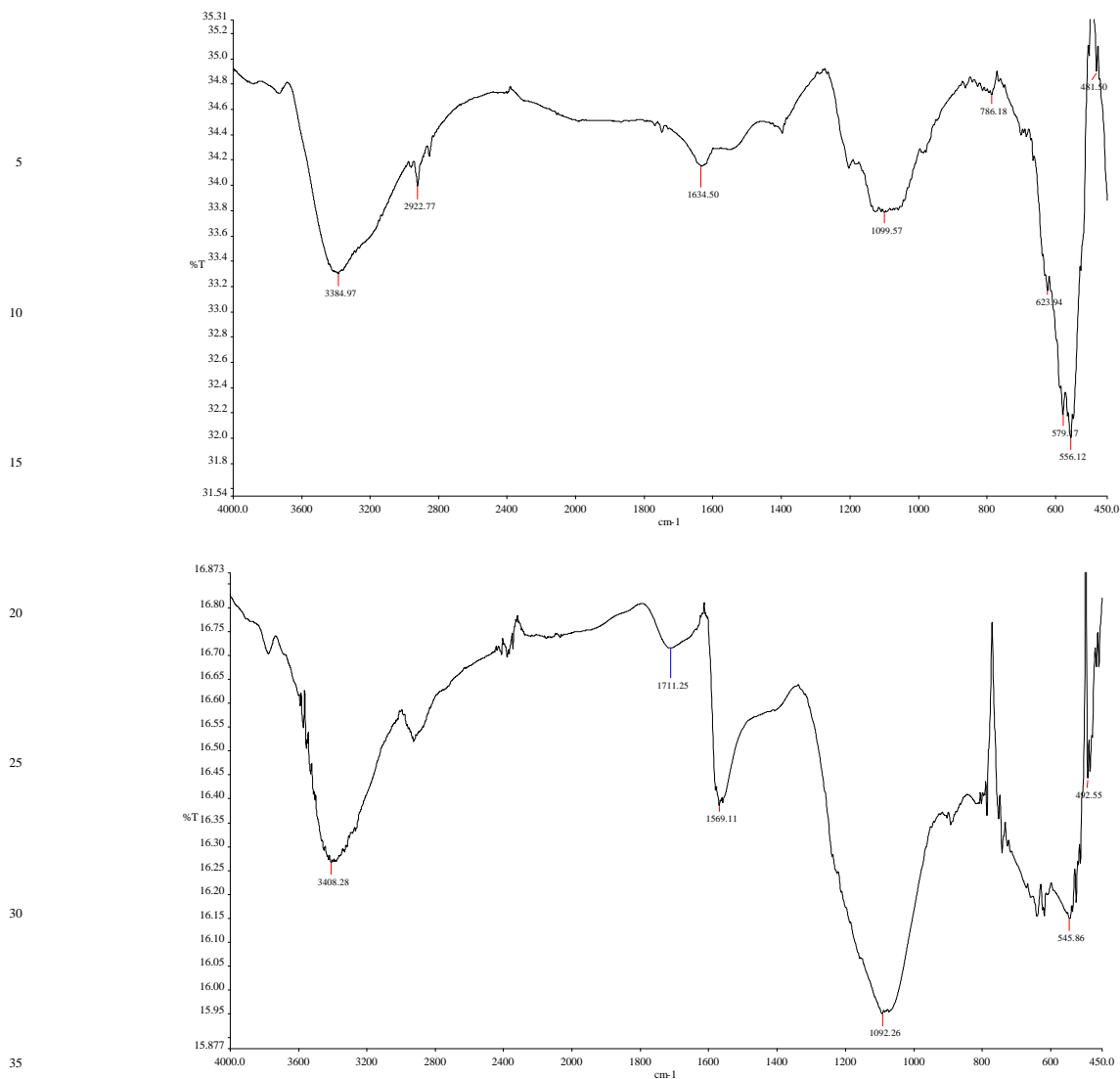
### FTIR Study

The FTIR spectra of GO and  $\text{GO-Fe}_3\text{O}_4$  hybrid are shown in Figs 1 and 2. The peak at 1711  $\text{cm}^{-1}$  corresponding to  $\nu(\text{C}=\text{O})$  of –COOH on the GO shifts to 1634  $\text{cm}^{-1}$  due to the formation of –

Cite this: DOI: 10.1039/c0xx00000x

www.rsc.org/xxxxxx

ARTICLE TYPE

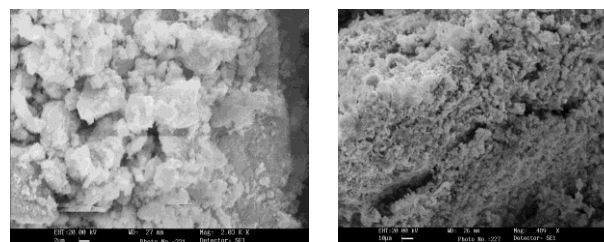
FT-IR spectra of (Fig. 1, top)  $\text{Fe}_3\text{O}_4$ -GO nanocomposite and (Fig. 2, bottom) graphene oxide

-COO<sup>-</sup> after coating with  $\text{Fe}_3\text{O}_4$ . The characteristic peak corresponding to the stretching vibration of Fe-O bond is also shifted to  $786.2\text{ cm}^{-1}$  compared to  $545.9\text{ cm}^{-1}$  reported for bulk  $\text{Fe}_3\text{O}_4$ ,<sup>27-29</sup> suggesting that  $\text{Fe}_3\text{O}_4$  is bound to the -COO<sup>-</sup> on the GO surface.

### SEM Study

In Fig 3, SEM images of iron oxide nanoparticles, and nanocomposites of iron oxide and graphene oxide (GO) are shown. The images are clearly distinguishable, with the image of iron oxide nanoparticles showing more cluster-like compositions having larger grains, and its nanocomposite with GO showing more uniform structure with smaller particles. In Fig 4(a), energy dispersive X-ray analysis (EDX) of  $\text{Fe}_3\text{O}_4$

nanoparticles and in Fig. 4(b) that of  $\text{Fe}_3\text{O}_4$ -GO nanocomposite are shown.

Fig. 3. SEM images of  $\text{Fe}_3\text{O}_4$  nanoparticles (left) and  $\text{Fe}_3\text{O}_4$ -GO nanocomposite (right)

Cite this: DOI: 10.1039/c0xx00000x

www.rsc.org/xxxxxx

ARTICLE TYPE

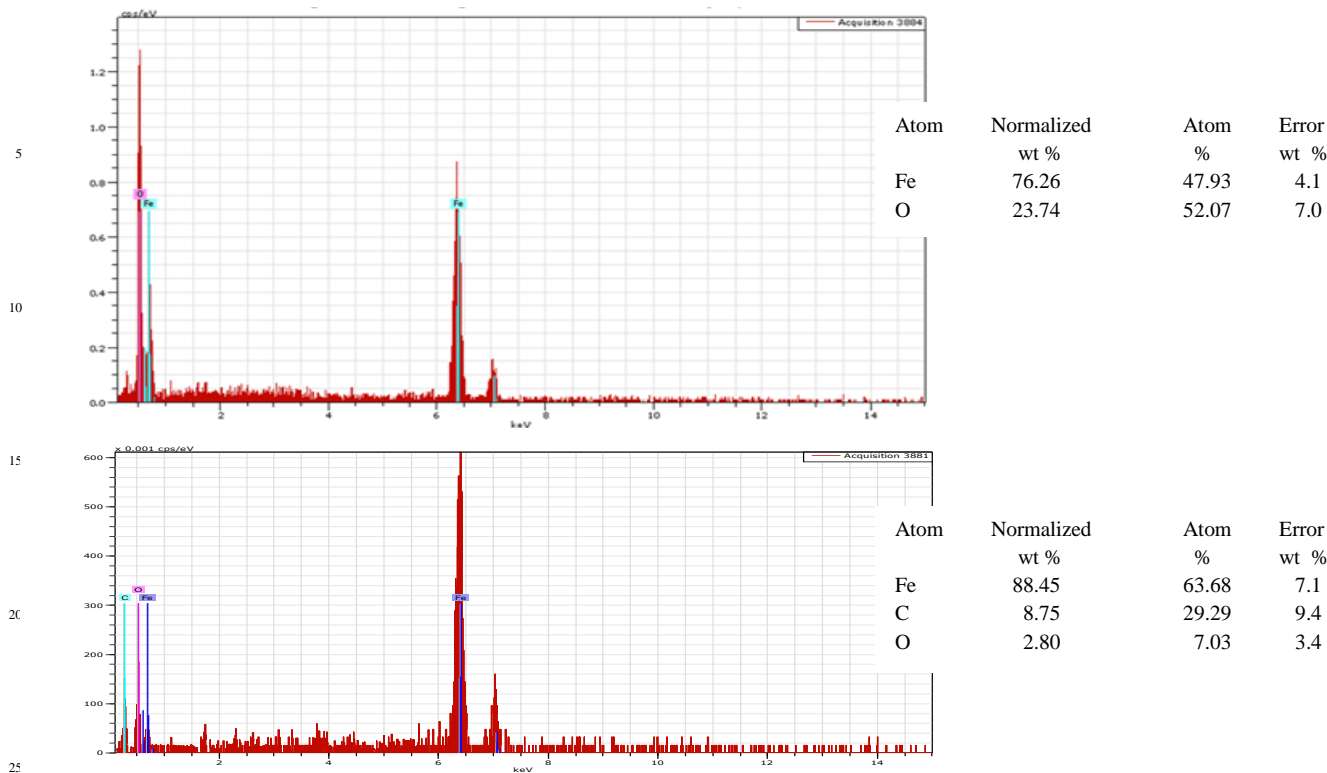


Fig. 4. EDX images of Fe<sub>3</sub>O<sub>4</sub> nanoparticles (top) and of Fe<sub>3</sub>O<sub>4</sub>-GO nanocomposites (bottom)

### XRD Study

Next, the powder XRD data of iron oxide-GO nanocomposite is presented in Fig. 5. The most striking feature is the typical graphene (002) signature at 26.6°. Usually, it is expected that, as graphene is oxidized to graphene oxide, this peak disappears and another one at much smaller angle (around 10-11°) appears. Also, as GO is made into a composite with metallic nanoparticles, the peak at 26.6° is supposed to become broader, with sharper peaks appearing at larger angles due to metal (or metal oxide). The peaks at 24.3°, 33.2° and 49.5° (marked in blue) may be ascribed to (012), (104) and (024) lines of α-haematite.<sup>30</sup> The peak at 30.6°, 35.7° and 41.1° may be identified as (220), (311) and (400) of Fe<sub>3</sub>O<sub>4</sub> (marked in red).<sup>10</sup> Thus, beside the peak at 26.6° of graphene (002), the broader peak centred at 43.5° is most probably composed of the (100) peak of graphene, which is usually followed immediately by the (101) peak.<sup>31</sup> This may explain the broadness of the peak. Please note that the (311) peak is expected to reduce much upon formation of composite with GO,<sup>10</sup> which is observed here. While the peak at 24.3° could also be ascribed to a different interplanar distance between graphene sheets, i.e. to the (002) peak usually observed at 26.6°, that would also lead to a much broader peak in this region,<sup>32</sup> which is not seen.

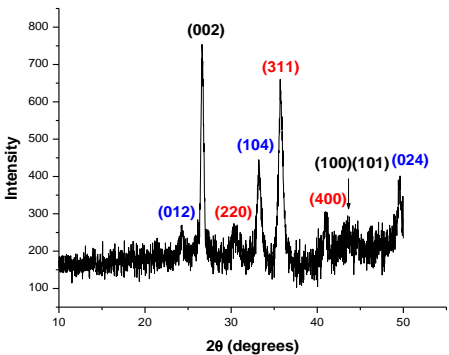


Fig. 5. Powder XRD spectrum of iron oxide GO nanocomposite. Black, red and blue denote GO, Fe<sub>3</sub>O<sub>4</sub> and α-Fe<sub>2</sub>O<sub>3</sub> respectively.

### TGA Study

We next present thermogravimetric analysis of iron oxide and iron oxide-graphene oxide nanocomposites. The TGA data of the two systems are shown in Fig. 6 below. The TGA curve of iron oxide nanoparticles show a 5% weight loss till 200 °C, followed by a further weight loss of 3.5% till 300 °C, and a slow loss of 1.5% from 300 °C to 800 °C. These indicate loss



of moisture, some of it more tightly bound. The curve for iron oxide-GO nanocomposite shows two shoulders, one around

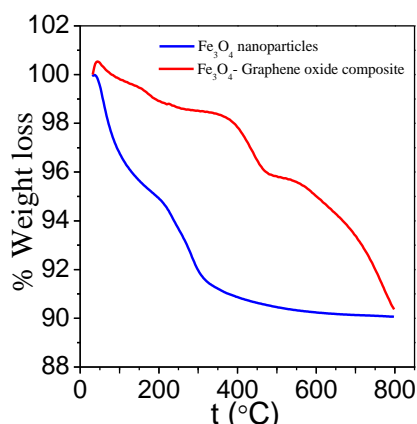


Fig. 6. Thermogravimetric analysis of  $\text{Fe}_3\text{O}_4$  nanoparticles and  $\text{Fe}_3\text{O}_4$ -GO nanocomposite

375 °C (wt loss 1.5%) and another ~535 °C (wt loss 2.7%). The remaining weight loss upto 800 °C is ~5.6%. This behaviour is clearly different from most known samples of GO, which show upto 15% wt loss till 100 °C<sup>33</sup> and over 30% wt loss beyond, in the 100-200 °C range.<sup>34</sup> The nanocomposite shows far greater stability upto 800 °C, most probably due to binding of iron oxide nanoparticles to the carboxylate groups etc. of GO platelets.

### TEM Study

Fig. 7 shows transmission electron micrographs of graphene oxide- $\text{Fe}_3\text{O}_4$  nanocomposites. Low magnification TEM images (Fig. 7(a) and (b)) reveals the clean images of small  $\text{Fe}_3\text{O}_4$  nanoparticles distributed homogeneously in the flexible two dimensional graphene oxide nanosheets. These images are the direct proof of the formation of graphene oxide- $\text{Fe}_3\text{O}_4$  nanocomposites. Moreover, high resolution TEM images (Fig. 7(c), (d) and (e)) shows high crystallinity of  $\text{Fe}_3\text{O}_4$  nanoparticles with the appearance of lattice fringes distributed in the graphene oxide nanosheets matrix. The distance between two lattice fringes are calculated by using the line profile (a line drawn to the perpendicular of lattice fringes) graph shown in Fig. 7(f). It shows that the distance between two lattice fringes is 0.252 nm which corresponds to the (311) plane of  $\text{Fe}_3\text{O}_4$  crystal. Interestingly, the distinction among the composites and the two constituents can be clearly made by analyzing the selected area electron diffraction (ED) patterns. Fig. 8 shows the ED patterns of  $\text{Fe}_3\text{O}_4$  nanoparticles, graphene oxide nanosheets and  $\text{Fe}_3\text{O}_4$ -GO nanocomposites. Fig. 8(a) shows the ED pattern of  $\text{Fe}_3\text{O}_4$  nanoparticles with the appearance of rings indicates the polycrystalline nature of the particles. Fig 8(b) shows the ED pattern of graphene oxide taken from a single sheet. Hexagonal ED pattern of GO indicates the single crystalline nature. Fig. 8(c) shows the ED pattern taken from a  $\text{Fe}_3\text{O}_4$ -GO composite. Both ring like ED pattern of  $\text{Fe}_3\text{O}_4$  nanoparticles and hexagonal ED pattern of

GO can be clearly observed. This fact suggests the formation of GO- $\text{Fe}_3\text{O}_4$  nanocomposites.

### Raman spectrum of the $\text{Fe}_3\text{O}_4$ -graphene oxide nanocomposite

Raman spectrum of the  $\text{Fe}_3\text{O}_4$ -graphene oxide nanocomposite is given below (Fig. 9). Characteristic peaks of  $\text{Fe}_3\text{O}_4$  alone, which are seen in the range 200 – 600  $\text{cm}^{-1}$ , are absent in the present spectrum. Only, the typical D and G peaks of graphene oxide are seen at 1355.5 and 1585  $\text{cm}^{-1}$  respectively. The  $I_D/I_G$  ratio is 1.037, showing onset of disorder induced by iron oxide.

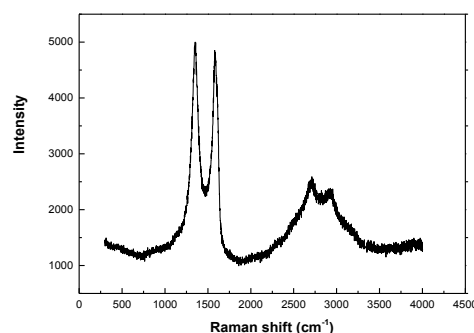


Fig. 9. Raman spectrum of  $\text{Fe}_3\text{O}_4$ -GO nanocomposite

The harmonics are also seen at 2711 and 3170  $\text{cm}^{-1}$ . Absence of the iron oxide peaks in Raman spectrum may indicate low concentration of  $\text{Fe}_3\text{O}_4$  particles in GO. The actual amount of  $\text{Fe}_3\text{O}_4$  in GO was ascertained by Atomic Absorption Spectroscopy (AAS) as 8.232% of  $\text{Fe}_3\text{O}_4$  in GO (w/w).<sup>35</sup>

### Catalytic activity

Propargylic amines, products of the  $A^3$ -coupling, are important synthetic intermediates for natural products and potential therapeutic agents.<sup>36</sup> There is some report of single  $\text{Fe}_3\text{O}_4$  nanoparticles catalyzing  $A^3$ -coupling.<sup>37,38</sup> As a comparison, we used graphene oxide- $\text{Fe}_3\text{O}_4$  nanocomposite as a catalyst in  $A^3$ -coupling reaction.

Optimization of the performance of the catalyst with different amounts of GO- $\text{Fe}_3\text{O}_4$  nanocomposite was carried out. The  $A^3$  coupling reaction of aryl aldehyde, amine and benzene alkyne was examined by various catalysts of varying amounts was examined (Table 1). In the absence of the nanocomposite, no  $A^3$  coupling product was observed (Table 1, entry 10). As expected, in the presence of catalyst, yield of the coupling product was 93% for 5 wt% loading of GO- $\text{Fe}_3\text{O}_4$  nanocomposite catalyst. The catalytic activity increased with the increase of the GO- $\text{Fe}_3\text{O}_4$  amount up to 5 wt% (Table 1, 1-7). On the other hand, in a control experiment when homogeneous phase  $\text{Fe}_3\text{O}_4$ , GO and an iron salt was used as the catalyst under optimized conditions, only 19%, 25% and 83% yields of the propargylamines (Table 1 Entry 8,9,11) were obtained. Thus GO- $\text{Fe}_3\text{O}_4$  nanocomposite catalyst was more efficient in  $A^3$  coupling reaction than the other substances used.

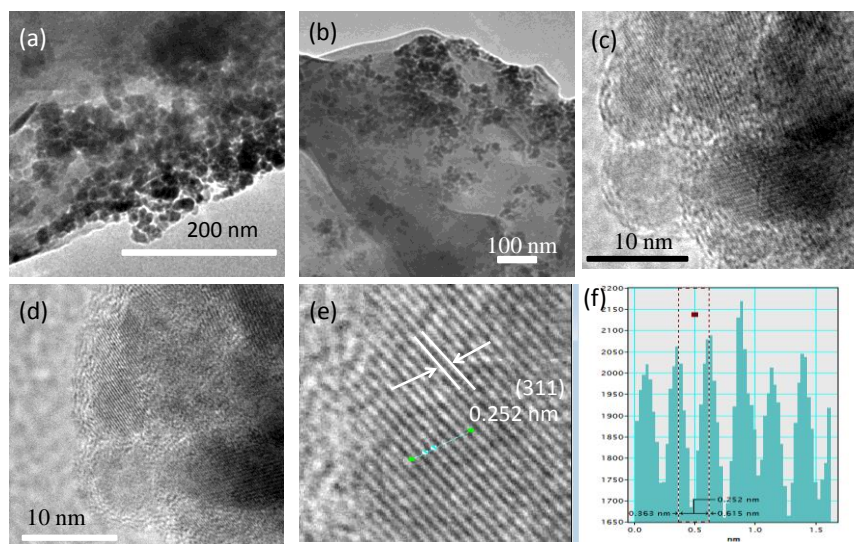


Fig. 7. (a) and (b) Low magnification TEM images, (c), (d) and (e) HRTEM images of graphene oxide- $\text{Fe}_3\text{O}_4$  nanocomposites. (f) Line profile of Fig. 6 (e)

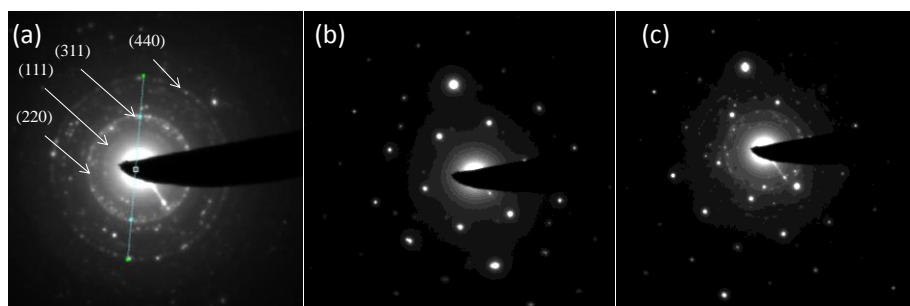
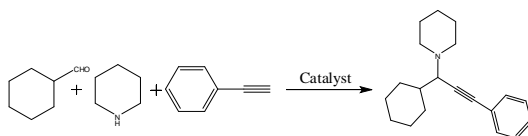


Fig. 8. (a), (b) and (c) Electron diffraction patterns of  $\text{Fe}_3\text{O}_4$ , graphene oxide and  $\text{Fe}_3\text{O}_4$ -graphene oxide nanocomposites respectively.

Table 1. Effect of catalyst in the 3-component coupling of cyclohexanecarbaldehyde, piperidine, and phenylacetylene.



Entry	Catalyst	Catalyst amt (g)	Yield (%)
1	GO- $\text{Fe}_3\text{O}_4$	0.0020	63
2	GO- $\text{Fe}_3\text{O}_4$	0.0025	70
3	GO- $\text{Fe}_3\text{O}_4$	0.0030	76
4	GO- $\text{Fe}_3\text{O}_4$	0.0035	81
5	GO- $\text{Fe}_3\text{O}_4$	0.0040	84
6	GO- $\text{Fe}_3\text{O}_4$	0.0045	89
7	GO- $\text{Fe}_3\text{O}_4$	0.0050	93
8	$\text{Fe}_3\text{O}_4$	0.0050	19
9	GO	0.0050	25
10	GO- $\text{Fe}_3\text{O}_4$	0.0000	trace
11	Salt of Iron	0.0100	83%

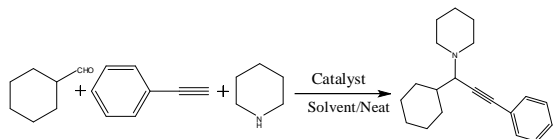
Conditions of the above reaction were as follows. Aldehyde (1 equiv), amine (1.2 equiv), alkyne (1.5 equiv) and GO- $\text{Fe}_3\text{O}_4$  (50mg, 0.3 mol%  $\text{Fe}_3\text{O}_4$  np) were taken in 5 mL solvent or neat for 16 h, at temperature above 90  $^{\circ}\text{C}$ .

Conversions were determined by GC-MS and  $^1\text{H}$  NMR analysis of crude reaction mixture.<sup>39</sup>

We also investigated the effects of reaction temperature, solvents and reaction time on the catalytic efficiency. At a lower reaction temperature (25  $^{\circ}\text{C}$ ), the GO- $\text{Fe}_3\text{O}_4$  nanocomposite (0.0050 mmol) showed lower conversion due to an incomplete reaction. We obtained excellent conversion at a higher reaction temperature (above 90  $^{\circ}\text{C}$ ). Solvent-free conditions proved to be the most effective for the  $\text{A}^3$ -coupling reaction (Table 2) and the conversion was comparable to that of the homogeneous catalyst (Table 1). As shown in Table 2, one could conclude from the influence of the reaction time on the activity that the  $\text{A}^3$ -coupling reaction reaches completion after 24 h under the present conditions. We obtained the products in moderate or low conversions when using ethanol, dichloromethane (DCM), *N,N*-dimethylformamide (DMF), tetrahydrofuran (THF), acetonitrile, dimethyl sulfoxide (DMSO), and ethyl acetate (Table 2). We also obtained slightly lower conversions when using water or toluene as the solvent (Table 2). The optimized reaction conditions include 0.5 equiv of aldehyde, 0.6 equiv of amine, 7.5 equiv of alkyne, and 0.0050 mmol of GO- $\text{Fe}_3\text{O}_4$  nanocomposite at 90  $^{\circ}\text{C}$ , solvent-free in air.



Table 2. Effects of various solvents in the 3-component coupling of cyclohexanecarbaldehyde, piperidine, and phenylacetylene catalyzed by the graphene-Fe<sub>3</sub>O<sub>4</sub> catalyst.



Entry	Solvent (ml)	Conversion (%)
1	Ethanol	48
2	DCM	70
3	DMF	Trace
4	THF	09
5	Acetonitrile	46
6	DMSO	44
7	ethyl acetate	Trace
8	Water	78
9	Toluene	84
10	Neat	93

On the other hand the reaction depends on temperature and time (data given in Supplementary Information). When reaction time increases, the product yield also increases in water and in solvent. In addition, it was found that at higher temperatures GO-Fe<sub>3</sub>O<sub>4</sub> nanocomposite show good catalytic activity; at 90 °C-120 °C, a 93% yield were obtained, however at room temperature lower yields are obtained even after longer reaction times.

To expand the scope of this A<sup>3</sup>-coupling, we used various aldehydes, alkynes, and amines were used as substrates under the optimized reaction conditions, and the results are summarized in Table 3. In general, both aliphatic and aromatic aldehydes underwent the addition reaction smoothly to provide the desired product in moderate to excellent yields. As shown in Table 3 (entry 1), only a trace of A<sup>3</sup>-coupling product was observed by NMR. Note that the reactions proceeded smoothly to give the corresponding propargylamines in a excellent yield. The presence of electron-rich groups on the benzene ring (Table 3, entries 2–5) increased the reactivities of the alkynes whereas electron-withdrawing groups (Table 3, entry 6) on the benzene decreased the yield. However, aliphatic aldehydes such as cyclohexanecarboxaldehyde, 2-ethylbutanal and formaldehyde all give both higher conversions and greater yields (Table 3, entries 7-10). It was important to notice that formaldehyde provides excellent yield than other carbon chain aliphatic aldehyde (Table 3, entry 10). Good yields were observed when cyclic dialkylamines such as pyrrolidine and morpholine were used (Table 3, entries 11 and 12).

The effect of electron-withdrawing groups on the alkyne was also investigated (Table 3, entries 13 and 14). For 2-ethynylpyridine and 2-ethynylthiophene, yields were 58% and 37% respectively. The reaction failed with 2-ethynylfuran. One problem could be the high volatility of the

reactants, which require low temperatures for storage, while our optimum condition was above 90 °C. We are currently investigating reaction with such substrates further.

We also investigated the effect of adding a mixture of GO and Fe<sub>3</sub>O<sub>4</sub> nanoparticles, instead of the nanocomposite, for the reaction of cyclohexanecarbaldehyde, piperidine and phenylacetylene. The yield obtained was 34.5%, less than for nanocomposite (Table 3, entry 7). Also, in O<sub>2</sub> and N<sub>2</sub> atmosphere, the yields of the same reaction were 62% and 75% respectively. This may be related to the stability of intermediate species involved.<sup>40, 41</sup>

### Catalyst recycling

The magnetically active GO-Fe<sub>3</sub>O<sub>4</sub> nanoparticles were adsorbed onto the magnetic stirring bar when the magnetic stirring was stopped. The nanoparticles were then washed with ethyl acetate, air-dried and used directly for the next round of reactions without further purification. It was shown that the nanocomposite catalyst could be recovered and reused 12 times without significant loss of catalytic activity (Table 4 and Fig. 10).

Table 4. The reuse of catalyst in A<sup>3</sup>-coupling

Cycle	% Yield by GC-MS	Cycle	% Yield by GC-MS
1	93	7	79
2	87	8	77
3	86	9	75
4	84	10	74
5	83	11	72
6	82	12	71

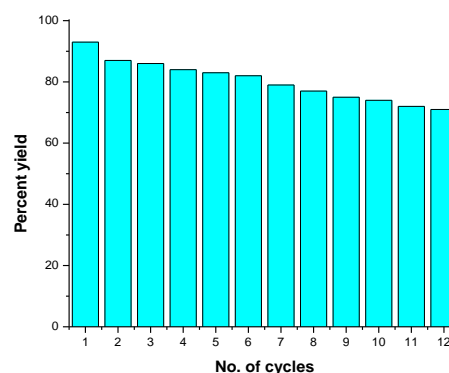


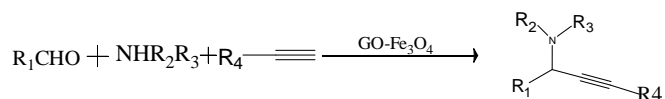
Fig. 10. Recycling of GO-Fe<sub>3</sub>O<sub>4</sub> (3 mol %) catalyst for the t A<sup>3</sup>-coupling of aldehyde, amine and alkyne in air in solvent-free conditions.

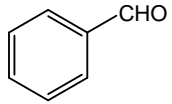
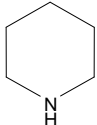
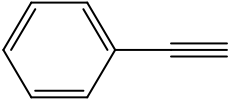
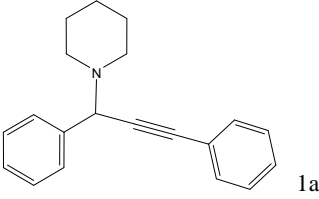
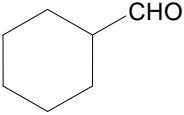
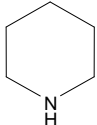
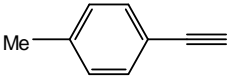
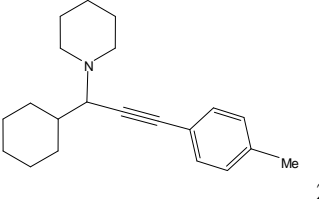
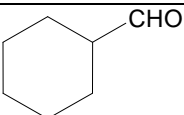
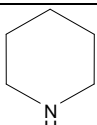
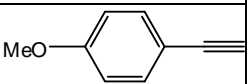
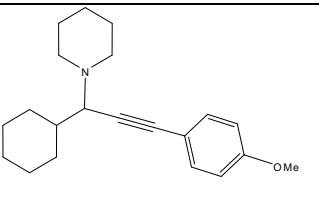
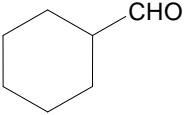
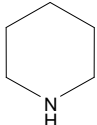
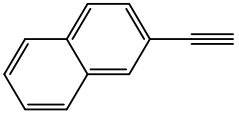
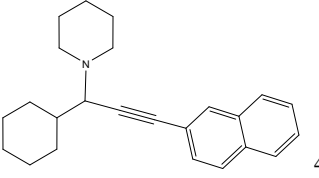
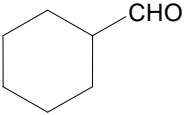
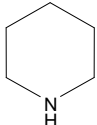
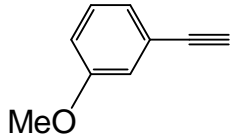
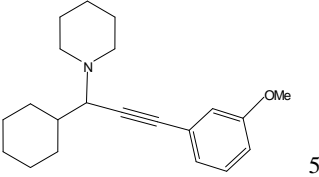
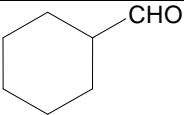
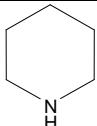
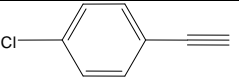
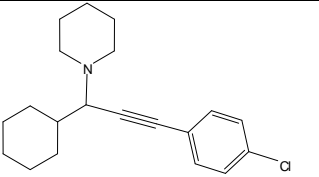
Further examination of the catalyst after recycling it 12 times in the above reaction produced interesting results. The FTIR and XRD spectra, given in Supplementary Information (Figs. S1 and S2) have the following general features.

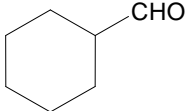
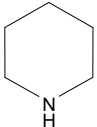
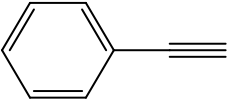
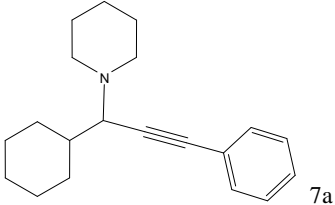
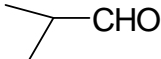
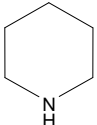
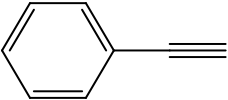
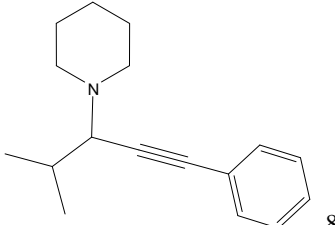
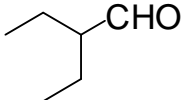
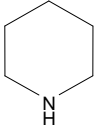
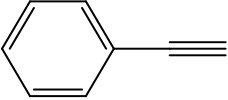
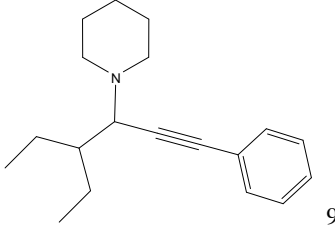
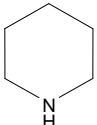
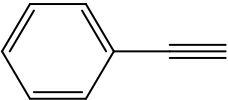
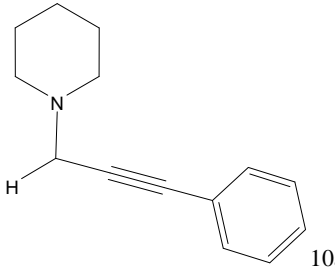
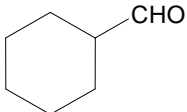
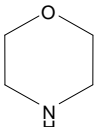
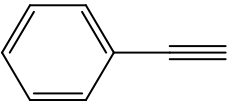
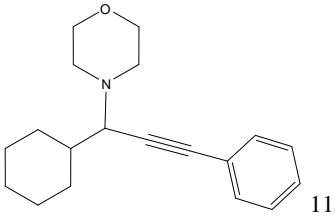
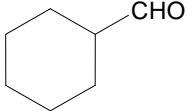
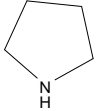
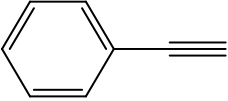
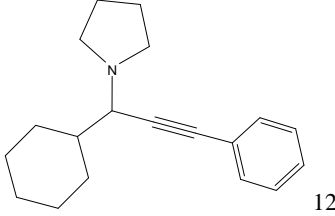
Cite this: DOI: 10.1039/C5DT0260K

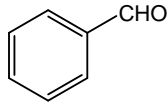
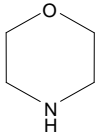
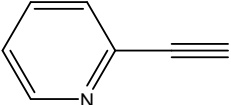
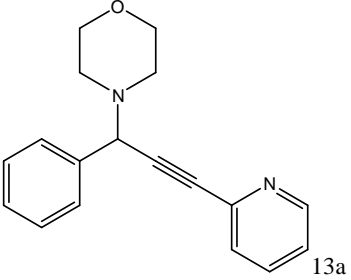
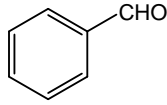
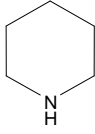
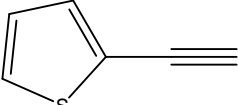
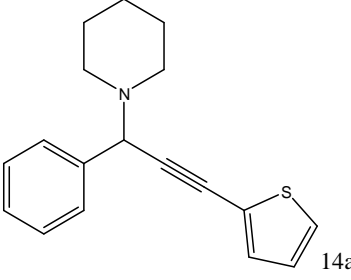
www.rsc.org/xxxxxx

## ARTICLE TYPE

Table 3. Effect of substituents on the Fe<sub>3</sub>O<sub>4</sub>-GO nanocomposite catalysed A<sup>3</sup> coupling reaction

Entry	Aldehyde	Amine	Alkyne	Product	Yield(%)
1				 1a	Trace
2				 2a	81
3				 3a	84
4				 4a	76
5				 5a	70
6				 6a	64

7				 7a	93
8				 8a	83
9				 9a	70
10	Formaldehyde			 10a	90
11				 11a	83
12				 12a	78

13					58
14					37

Most notably, the Fe-O bond, at  $786.2\text{ cm}^{-1}$  in pristine  $\text{Fe}_3\text{O}_4$ -GO nanocomposite, shifts to  $772.50\text{ cm}^{-1}$  (Fig. S1 in Supplementary Information). This shows that the Fe—O is weakened after recycling the nanocomposite 12 times, but is still intact. This is true of other features of the nanocomposite (See Figs. S1 and S2 in Supplementary Information). In other words, the essential features of the nanocomposite remain intact after recycling a dozen times.

## Conclusion

Nanocomposites of graphene oxide, doped with  $\text{Fe}_3\text{O}_4$  nanoparticles, were prepared by a simple and robust method. These particles were characterized by the usual manner. They display excellent catalytic activity, which was used in the one-pot synthesis of propargylamines following the  $\text{A}^3$ -coupling protocol. Magnetic behaviour of the nanocomposites may be employed to reuse the catalyst. Currently, we are engaged in examining how both product yield and catalyst life may be increased using easily available means.

## Characterization of compounds

### 1-(1,3-diphenylprop-2-ynyl)piperidine (1a)

$^1\text{H}$  NMR ( $\text{CDCl}_3$ , 250 MHz)  $\delta$ : 1.57-1.63 (m, 2H), 1.72-1.83 (m, 4H), 2.71-2.73 (m, 4H), 4.96 (s, 1H), 7.42-7.53 (m, 6H), 7.66-7.69 (m, 2H), 7.82 (d,  $j = 7.2\text{ Hz}$ , 2H),

### 1-[1-Cyclohexyl-3-(4-methylphenyl)-2-propynyl]piperidine (2a)

H-NMR ( $\text{CDCl}_3$ , 400MHz):  $\delta$  7.30 (d, 2H), 7.06 (d, 2H), 3.08 (d, 1H), 2.66-2.58 (m, 2H), 2.40-2.32 (m, 2H), 2.30 (s, 3H), 2.10-1.96 (m, 2H), 1.77-1.67 (m, 2H), 1.64-1.47 (m, 6H), 1.44-1.35 (m, 2H), 1.31-1.10 (m, 3H), 1.06-0.88 (m, 2H),

### 1-(1-cyclohexyl-3-(4-methoxyphenyl) prop-2-ynyl)piperidine (3a)

$^1\text{H}$ -NMR (400MHz,  $\text{CDCl}_3$ ):  $\delta$ = 7.36 (d, 2H), 6.80 (d, 2H), 3.81 (s, 3H), 3.07 (d, 1H), 2.65-2.58 (m, 2H), 2.38 (br, 2H), 2.10-2.02 (m, 2H), 1.76-1.56 (m, 8H), 1.45-1.40 (m, 2H), 1.30-1.01 (m, 3H), 1.00-0.86 (m, 2H),

### 1-(1-cyclohexyl-3-(3-methoxyphenyl)-prop-2-ynyl)piperidine (4a)

H-NMR (400MHz,  $\text{CDCl}_3$ ):  $\delta$ = 7.20-7.17 (m, 1H), 7.05 (d, 1H), 6.97 (d, 1H), 6.81-6.80 (d, 1H), 3.81 (s, 3H), 3.10 (d, 1H), 2.63-2.58 (m, 2H), 2.38 (br, 2H), 2.10-2.01 (m, 2H), 1.76-1.53 (m, 8H), 1.45-1.40 (m, 2H), 1.31-1.01 (m, 3H), 1.01-0.85 (m, 2H)

### 1-(3-(4-chlorophenyl)-1-cyclohexylprop-2-ynyl)piperidine (5a)

H-NMR (400MHz,  $\text{CDCl}_3$ ):  $\delta$ = 7.34 (d, 2H), 7.27 (d, 2H), 3.07 (d, 1H), 2.60-2.57 (m, 2H), 2.36 (br, 2H), 2.07-2.00 (m, 2H), 1.84-1.73 (m, 2H), 1.66-1.50 (m, 6H), 1.45-1.40 (m, 2H), 1.32-1.13 (m, 3H), 1.04-0.85 (m, 2H)

### 1-(1-Cyclohexyl-3-phenyl-2-propynyl)piperidine (6a)

H-NMR ( $\text{CDCl}_3$ , 400MHz, ppm):  $\delta$  7.46-7.44 (m, 2H), 7.30-7.24 (m, 3H), 3.09 (d, 1H), 2.65-2.60 (m, 2H), 2.44-2.40 (m, 2H), 2.14-2.04 (m, 2H), 1.80-1.70 (m, 2H), 1.65-1.51 (m, 6H), 1.45-1.40 (m, 2H), 1.34-1.15 (m, 3H), 1.07-0.88 (m, 2H).

### N-(1-Isopropyl-3-phenyl-2-propynyl) piperidine (7a)

H-NMR ( $\text{CDCl}_3$ , 400MHz, ppm):  $\delta$ = 7.47-7.44 (m, 2H), 7.34-7.30 (m, 3H), 3.01 (d, 1H), 2.69-2.65 (m, 2H), 2.43 (br, 2H), 1.97-1.93 (m, 1H), 1.68-1.57 (m, 4H), 1.49-1.46 (m, 2H), 1.10 (d, 3H), 1.02 (d, 3H).

### 1-[1-(1-Ethylpropyl)-3-phenyl-2-propynyl] piperidine (8a)

H-NMR ( $\text{CDCl}_3$ , 400MHz, ppm):  $\delta$ = 7.44-7.41 (m, 2H), 7.33-7.23 (m, 3H), 3.21 (d, 1H), 2.65-2.61 (m, 2H), 2.43-2.39 (m, 2H), 1.78-1.65 (m, 1H), 1.61-1.50 (m, 6H), 1.51-1.40 (m, 4H), 0.91 (t, 3H), 0.83 (t, 3H)

### N-(3-Phenyl)-prop-2-ynyl piperidine (9a)

<sup>1</sup>H-NMR (CDCl<sub>3</sub>, 400MHz, ppm): δ= 7.44-7.42 (m, 2H), 7.31-7.28 (m, 3H), 3.47 (s, 2H), 2.56 (br, 4H), 1.69-1.60 (m, 4H), 1.45 (br, 2H).

#### 4-(1,3-Diphenyl-prop-2-ynyl)-morpholine (10a)

<sup>1</sup>H NMR (300 MHz, CDCl<sub>3</sub>): δ 7.63 (d, J = 6.9 Hz, 2H), 7.50 (d, J = 6.9 Hz, 2H), 7.36-7.31 (m, 6H), 4.78 (s, 1H), 3.71-3.64 (m, 4H), 2.62-2.56 (m, 4H);

#### 1-[1-Cyclohexyl-3-phenyl-2-propynyl] pyrrodine (11a)

<sup>1</sup>H-NMR (CDCl<sub>3</sub>, 400MHz, ppm): δ= 7.43-7.42 (m, 2H), 7.31-7.24 (m, 3H), 3.33 (d, 1H), 2.74-2.70 (m, 2H), 2.64-2.63 (m, 2H), 2.08 (d, 1H), 1.94 (d, 1H), 1.75-1.74 (m, 6H), 1.68-1.64 (m, 1H), 1.60-1.51 (m, 1H), 1.31-1.04 (m, 5H). Besides these, <sup>1</sup>H-NMR and HRMS data of several products are given in Supplementary Information.<sup>42</sup>

## Acknowledgements

The authors would like to acknowledge help and assistance received from Prof. K. Ghosh of the Dept. of Chemistry, and from Prof. T. Basu of the Dept. of Biochemistry & Biophysics, University of Kalyani. Help from DST-FIST, DST-PURSE programs are gratefully acknowledged. PM acknowledges financial support from RGNF from UGC, New Delhi. Prof. A. Kaviraj, Dept. Of Zoology, University of Kalyani must be acknowledged for help with AAS. The authors gratefully acknowledge suggestions from the anonymous referees, which not only improved the content, but also pointed to new lines of investigation, esp. with substituted alkynes.

## References

- 1 C. Cao, Y. Shi and A. L. Odom, *J. Am. Chem. Soc.*, 2003, 125, 2880-2881; S. Kamijo and Y. Yamamoto, *J. Am. Chem. Soc.*, 2002, 124, 11940-11945; A. Domling and I. Ugi, *Angew. Chem.*, 2000, 112, 3300-3344; I. Ugi, A. Domling and B. Werner, *J. Heterocycl. Chem.*, 2000, 37, 647-658; R. W. Armstrong, A. P. Combs, P. A. Tempst, S. D. Brown and T. A. Keating, *Acc. Chem. Res.*, 1996, 29, 123-131.
- 2 For representative reviews on multi-component reactions, see: (a) J. Zhu and H. Bienayme (Eds.), *Multicomponent Reaction*, Wiley-VCH, Weinheim, 2005; (b) G. H. Posner, *Chem. Rev.*, 1986, 86, 831-844; (c) A. Domling, *Chem. Rev.*, 2006, 106, 17-89; (d) D. M. D'Souza and T. J. J. Muller, *Chem. Soc. Rev.*, 2007, 36, 1095-1108; (e) D. Tejedor and F. Garcia-Tellado, *Chem. Soc. Rev.*, 2007, 36, 484-491; (f) B. Ganem, *Acc. Chem. Res.*, 2009, 42, 463-472.
- 3 (a) G. S. Kauffman, G. D. Harris, R. L. Dorow, B. R. P. Stone, R. L. Parsons, Jr., J. A. Pesti, N. A. Magnus, J. M. Fortunak, P. N. Confalone and W. A. Nugent, *Org. Lett.*, 2000, 2, 3119-3121; (b) M. A. Huffman, N. Yasuda, A. E. DeCamp and E. J. J. Grabowski, *J. Org. Chem.*, 1995, 60, 1590-1594; (c) M. Konishi, H. Ohkuma, T. Tsuno, T. Oki, G. D. Van Duyne and J. Clardy, *J. Am. Chem. Soc.*, 1990, 112, 3715-3716.
- 4 (a) Y. Mori and H. Hayashi, *Tetrahedron*, 2002, 58, 1789-1797; (b) C. V. Galliford, M. A. Beenen, S. T. Nguyen and K. A. Scheidt, *Org. Lett.*, 2003, 5, 3487-3490; (c) C. I.

- Garcia, A. Tillack, C. G. Hartung and M. Beller, *Tetrahedron Lett.*, 2003, 44, 3217-3221
- 5 (a) M. A. Youngman and S. L. Dax, *J. Comb. Chem.*, 2001, 3, 469-472; (b) S. L. Dax, M. A. Youngman, P. Kocis and M. North, *Solid-Phase Org. Synth.*, 2001, 1, 45-53; (c) A. B. Dyatkin and R. A. Rivero, *Tetrahedron Lett.*, 1998, 39, 3647-3650; (d) J. J. McNally, M. A. Youngman and S. L. Dax, *Tetrahedron Lett.*, 1998, 39, 967-970; (e) M. A. Youngman and S. L. Dax, *Tetrahedron Lett.*, 1997, 38, 6347-6350.
- 6 (a) G. W. Kabalka, L. Wang and R. M. Pagni, *Synlett*, 2001, 5, 676-678; (b) A. Sharifi, H. Farhangian, F. Mohsenzadeh and M. R. Naimijamal, *Monatsh. Chem.*, 2002, 133, 199-204; (c) L. Wang and P.-H. Li, *Chin. J. Chem.*, 2003, 21, 710-713
- 7 (a) C. Wei, J. T. Mague and C.-J. Li, *Proc. Natl. Acad. Sci. U. S. A.*, 2004, 101, 5749-5754; (b) C. Wei and C.-J. Li, *Chem. Commun.*, 2002, 268-269; C. Wei, Z. Li and C.-J. Li, *Synlett*, 2004, 1472-1483; Y. Ju, C.-J. Li and R. S. Varma, *QSAR Comb. Sci.*, 2004, 23, 891-894.
- 8 C. Wei and C.-J. Li, *J. Am. Chem. Soc.*, 2003, 125, 584-9585.
- 9 C. Wei, Z. Li and C.-J. Li, *Org. Lett.*, 2003, 5, 4473-4475; Z. Li, C. Wei, L. Chen, R. S. Varma and C.-J. Li, *Tetrahedron Lett.*, 2004, 45, 2443-2446.
- 10 S. Satoshi, K. Takashi and Y. Ishii, *Angew. Chem., Int. Ed.*, 2001, 40, 2534-2536.
- 11 For examples, see: (a) V. Polshettiwar, B. Baruwati and R. S. Varma, *Chem. Commun.*, 2009, 1837-1839; (b) S. Luo, X. Zheng, H. Xu, X. Mi, L. Zhang and J.-P. Cheng, *Adv. Synth. Catal.*, 2007, 349, 2431-2434; (c) V. Polshettiwar, B. Baruwati and R. S. Varma, *Green Chem.*, 2009, 11, 127-131; (d) M. Kotani, T. Koike, K. Yamaguchi and N. Mizuno, *Green Chem.*, 2006, 8, 735-741; (e) D.-H. Zhang, G.-D. Li, J.-X. Lia and J.-S. Chen, *Chem. Commun.*, 2008, 3414-3416; (f) M. Kawamura and K. Sato, *Chem. Commun.*, 2006, 4718-4719; (g) M. Kawamura and K. Sato, *Chem. Commun.*, 2007, 3404-3405; (h) A. Hu, G. T. Yee and W. Lin, *J. Am. Chem. Soc.*, 2005, 127, 12486-12487; (i) G. Chouhan, D. Wang and H. Alper, *Chem. Commun.*, 2007, 4809-4811; (j) R. Abu-Reziq, D. Wang, M. Post and H. Alper, *Adv. Synth. Catal.*, 2007, 349, 2145-2150; (k) V. Polshettiwar and R. S. Varma, *Chem.-Eur. J.*, 2009, 15, 1582-1586; (l) J. Ge, Q. Zhang, T. Zhang and Y. Yin, *Angew. Chem., Int. Ed.*, 2008, 47, 8924-8928
- 12 M. Kidwai, V. Bansal, A. Kumar and S. Mozumdar, *Green Chem.*, 2007, 9, 742-745
- 13 A. Teimouri, A. N. Chermahini, M. Nariman 1556 *Bull. Korean Chem. Soc.*, 2012, 33, 1556-1560
- 14 V. Chandra, J. Park, Y. Chun, J. W. Lee, I. C. Hwang and K. S. Kim, *ACS Nano*, 2010, 4, 3979-3986
- 15 Y. Zhang, B. Chen, L. Zhang, J. Huang, F. Chen and Z. Yang, *Nanoscale*, 2011, 36, 1446-1450
- 16 (a) S. Ikegami and H. Hamamoto, *Chem. Rev.* 2009, 109, 583-593; (b) J. Lu and P. H. Toy, *Chem. Rev.* 2009, 109, 815838
- 17 (a) G. M. Scheuermann, L. Rumi, P. Steurer, W. Bannwarth and R. Mulhaupt, *J. Am. Chem. Soc.* 2009, 131,



- 8262-8270; (b) N. R. Shiju and V. V. Guliants, *Appl. Catal. A: Gen.* 2009, 356, 1-17; (c) L. D. Pachon and G. Rothenberg, *Appl. Organomet. Chem.* 2008, 22, 288-299
- 18** (a) V. Polshettiwar and R. S. Varma, *Tetrahedron*, 2010, 66, 1091-1097; (b) K. Wang, L. X. Yu, S. Yin, H. Li and H. Li, *Pure Appl. Chem.* 2009, 81, 2327-2335; (c) W. Liu, B. J. Li, C. L. Gao and Z. Xu, *Chem. Lett.* 2009, 38, 1110-1111; (d) D. Rosario-Amorin, X. Wang, M. Gaboyard, R. Clerac, S. Nlate and K. Heuze, *Chem.-Eur. J.* 2009, 15, 12636-12643; (e) F. Shi, M. K. Tse, S. L. Zhou, M. M. Pohl, J. Radnik, S. Hubner, K. Jahnisch, A. Bruckner and M. Beller, *J. Am. Chem. Soc.* 2009, 131, 1775-1779; (f) M. J. Aliaga, D. J. Ramon and M. Yus, *Org. Biomol. Chem.* 2010, 8, 43-46; (g) X. J. Wu, R. Jiang, B. Wu, X. M. Su, X. P. Xu and S. J. Ji, *Adv. Synth. Catal.* 2009, 351, 3150-3156; (h) L. Lartigue, K. Oumzil, Y. Guari, J. Larionova, C. Guerin, J. L. Montero, V. Barragan-Montero, C. Sangregorio, A. Caneschi, C. Innocenti, T. Kalaivani, P. Arosio and A. Lascialfari, *Org. Lett.* 2009, 11, 2992-2995. (i) C. Che, W. Z. Li, S. Y. Lin, J. W. Chen, J. Zheng, J. C. Wu, Q. X. Zheng, G. Q. Zhang, Z. Yang, Z. and B. W. Jiang, *Chem. Commun.* 2009, 5990-5992; (j) K. Mori, N. Yoshioka, Y. Kondo, T. Takeuchi and H. Yamashita, *Green Chem.* 2009, 11, 1337-1342; (k) Y. H. Zhu, L. P. Stubbs, F. Ho, R. Z. Liu, C. P. Ship, J. A. Maguire and N. S. Hosmane, *Chemcatchem* 2010, 2, 365-374; (l) S. Shylesh, V. Schu"nemann, W. R. Thiel, *Angew. Chem., Int. Ed.* 2010, 49, 3428-3459; (m) T. Q. Zeng, W. W. Chen, C. M. Cirtiu, A. Moores, G. H. Song and C. J. Li, *Green Chem.* 2010, 12, 570-573; (n) B. Sreedhar, A. S. Kumar and P. S. Reddy, *Tetrahedron Lett.* 2010, 51, 1891-1895
- 19** J. Zhang, J. Wang, T. Lin, C. H. Wang, K. Ghorbani, J. Fang and X. Wang, *Chem. Engg. J.*, 2013, 237, 462-468
- 20** (a) A. J. Amali and R. K. Rana, *Green Chem.* 2009, 11, 1781-1786; (b) B. Baruwati, V. Polshettiwar and R. S. Varma, *Tetrahedron Lett.* 2009, 50, 1215-1218; (c) M. L. Kantam, J. Yadav, S. Laha, P. Srinivas, B. Sreedhar and F. Figueras, *J. Org. Chem.* 2009, 74, 4608-4611; (d) V. Polshettiwar and R. S. Varma, *Chem.-Eur. J.* 2009, 15, 1582-1586; (e) V. Polshettiwar and R. S. Varma, *Org. Biomol. Chem.* 2009, 7, 37-40; (f) S. Shylesh, J. Schweizer, S. Demeshko, V. Schunemann, S. Ernst and W. R. Thiela, *Adv. Synth. Catal.* 2009, 351, 1789-1795; (g) A. Taber, J. B. Kirn, J. Y. Jung, W. S. Ahn and M. J. Jin, *Synlett* 2009, 2477-2482; (h) B. Baruwati, D. Guin and S. V. Manorama, *Org. Lett.* 2007, 9, 5377-5380; (i) H. Georgey, N. Abdel-Gawad and S. Abbas, *Molecules* 2008, 13, 2557-2569; (j) D. Guin, B. Baruwati and S. V. Manorama, *Org. Lett.* 2007, 9, 1419-1421; (k) T. Hara, T. Kaneta, K. Mori, T. Mitsudome, T. Mizugaki, K. Ebitani and K. Kaneda, *Green Chem.* 2007, 9, 1246-1251; (l) A. G. Hu, G. T. Yee and W. B. Lin, *J. Am. Chem. Soc.* 2005, 127, 12486-12487; (m) V. Polshettiwar, B. Baruwati and R. S. Varma, *Green Chem.* 2009, 11, 127-131; (n) L. M. Rossi, F. P. Silva, L. L. R. Vono, P. K. Kiyohara, E. L. Duarte, R. Itri, R. Landers and G. Machado, *Green Chem.* 2007, 9, 379-385; (o) L. M. Rossi, L. L. R. Vono, F. P. Silva, P. K. Kiyohara, E. L. Duarte and J. R. Matos, *Appl. Catal. A: Gen.* 2007, 330, 139-144
- 21** (a) H. C. Hailes, *Org. Process Res. Dev.* 2007, 11, 114-120; (b) B. Jiang, L. J. Cao, S. J. Tu, W. R. Zheng and H. Z. Yu, *J. Comb. Chem.* 2009, 11, 612-616; (c) S. J. Tu, X. H. Zhang, Z. G. Han, X. D. Cao, S. S. Wu, S. Yan, W. J. Hao, G. Zhang and N. Ma, *J. Comb. Chem.* 2009, 11, 428-432; (d) H. Wu, W. Lin, Y. Wan, H. Q. Xin, D. Q. Shi, Y. H. Shi, R. Yuan, R. C. Bo and W. Yin, *J. Comb. Chem.* 2010, 12, 31-34
- 22** (a) Y.-H. Liu, Z.-H. Zhang and T. S. Li, *Synthesis* 2008, 3314-3318; (b) Z.-H. Zhang and X.-Y. Tao, *Aust. J. Chem.* 2008, 61, 77-79; (c) Y.-H. Liu, Q.-S. Liu and Z.-H. Zhang, *J. Mol. Catal. A: Chem.* 2008, 296, 42-46; (d) Y.-H. Liu, Q.-S. Liu and Z.-H. Zhang, *Tetrahedron Lett.* 2009, 50, 916-921; (e) P. Zhang and Z. H. Zhang, *Monatsh. Chem.* 2009, 140, 199-203
- 23** A. Bandyopadhyay, S. Chatterjee and K. Sarkar, *Current Science*, 2011, 101, 210-214
- 24** Y. Jiang, G. Li, Xiaodi Li, Lu Shuxiang, Li Wanga and X Zhanga, *J. Mater. Chem. A*, 2014, 2, 4779-4787
- 25** (a) W. S. Hummers Jr. and R. E. Offeman, *J. Am. Chem. Soc.*, 1958, 80, 1339-1339; (b) J. Song, X. Wang and C-T. Chang, *J. Nanomaterials* 2014, dx.doi.org/10.1155/2014/276143
- b) S. Guo and S. Dong, *Chem. Soc. Rev.*, 2011, 40, 2644-2672
- 26** L. Mancheng, C. Chen, J. Hu, X. Wu, X. Wang, *J. Phys. Chem. C*, 2011, 115, 25234-25240
- 27** X. Yang, X. Zhang, Y. Ma, Y. Huang, Y. Wang, *J. Mater. Chem.*, 2009, 19, 2710-2714
- 28** F. Chin, K. S. Iyer and C. L. Raston, *Lab Chip*, 2008, 8, 439-442
- 29** C. Rocchiccioli-Deltche, R. Franck, V. Cabuil and R. Massart, *J. Chem. Res.*, 1987, 5, 126
- 30** M. N. Batin and V. Popescu, *Powder Metallurgy Prog.*, 2011, 11, 201-205; B. Basly, D. Felder-Flesch, P. Perriat, C. Billotey, J. Taleb, G. Pourroy and S. Begin-Colin, *Chem. Commun.*, 2009, 46, 985-987
- 31** G. Wang, J. Yang, J. Park, X. Gou, B. Wang, H. Liu and J. Yao, *J. Phys. Chem. C*, 2008, 112, 8192-8195
- 32** Z.-S. Wu, W. Ren, L. Gao, J. Zhao, Z. Chen, B. Liu, D. Tang, B. Yu, C. Jiang and H.-M. Cheng, *ACS Nano*, 2009, 3, 411-417
- 33** C. Srinivasan and R. Saraswathi, *Curr. Sci.*, 2009, 97, 1115-1116
- 34** L. Zhang, J. Liang, Y. Huang, Y. Ma, Y. Wang and Y. Chen, *Carbon*, 2009, 47, 3365-3380
- 35** AAS was done on a Spectra AA 240 instrument (Agilent Tech.), with Ar/acetylene as carrier gas, and Fe was monitored at 372 nm.
- 36** (a) L. Zani and C. Bolm, *Chem. Commun.*, 2006, 4263-4275; (b) V. V. Kouznetsov and M. Vargas, *Synthesis*, 2008, 491-506; (c) V. A. Peshkov, O. P. Pereshivko and E. V. Van der Eycken, *Chem. Soc. Rev.*, 2012, 41, 3790-3807
- 37** T. Zeng, W.-W. Chen, C. M. Cirtiu, A. Moores, G. Song and C.-J. Li, *Green Chem.*, 2010, 12, 570-573
- 38** X. Huo, J. Liu, B. Wang, H. Zhang, Z. Yang, X. She and P. Xi, *J. Mater. Chem. A*, 2013, 1, 651-656

**39** Reaction products were quantified using a Varian 3400 Gas Chromatograph equipped with a 30-m CP-SIL8CB capillary column and flame ionization detector and identified by Trace DSQII GC equipped with a 60-m TR-50 MS capillary column

**40** A. Berrichi, R. Bachir, M. Benabdallah and N. Choukchou-Braham, *Tetrahedron Lett.*, 2015, 56, 1302-1306

**41** J. Lim, K. Park, A. Byeun and S. Lee, *Tetrahedron Lett.*, 2014, 55, 4875-4878

**42**  $^1\text{H}$  NMR spectra (Fig. S3 - Fig. S12, Supplementary Information) were recorded on a Bruker DRX-300A VANCE Spectrometer, with  $\text{CDCl}_3$  as solvent and TMS as the internal standard. HRMS spectra of 13a and 14a (the last two products) (Fig. S13 and S14, Supplementary Information) were taken with a Xevo G2-SQToF Mass Spectrometer (Waters).